**Supplementary Information (SI) for Materials Horizons.**

**This journal is © The Royal Society of Chemistry 2025**

## Supplementary Information

# Physically Programmed Vegan Leather Emulating the Mechanical and Sensory Characteristics of Animal Leather from Once-Discarded Gluten

Soyeon Kim,[ae] Jimin Choi,[b] Somyung Lee,[b] Dong Soo Hwang,[b] Giyoung Shin,[c] Jeyoung Park,[d*] and Dongyeop X. Oh[ae*]

[a] Department of Polymer Science and Engineering and Program in Environmental and Polymer Engineering, Inha University, Incheon 22212, Republic of Korea

E-mail: d.oh@inha.ac.kr

[b] Division of Environmental Science and Engineering, Pohang University of Science and Technology, Pohang, Republic of Korea

[c] Research Center for Bio-based Chemistry, Korea Research Institute of Chemical Technology (KRICT), Ulsan, 44429, Republic of Korea

[d] Department of Chemical and Biomolecular Engineering, Sogang University, Seoul 04107, Republic of Korea

E-mail: jeypark@sogang.ac.kr

[e] Division Department of Materials Science and Engineering, Korea University, Seoul 02841, Republic of Korea

E-mail: dongyeopoh@korea.ac.kr

# Table of Contents

# Experimental Section

## Materials

Wheat vital gluten (protein 100%) was purchased from Sigma-Aldrich. Glycerol (99%, EP) and iron(lll) chloride hexahydrate (98%, EP) were obtained from Duksan Pure Chemical Co., Ltd. (Korea). Tannic acid (ACS reagent) was purchased from Sigma-Aldrich. All chemical reagents were used as received.

## Preparation of WG-vegan leather

A brief fabrication procedure for WG-vegan leather is as follows. WG was employed to mimic the protein structure of animal leather. Because films composed solely of WG were too brittle, glycerol was added as a plasticizer. Glycerol, a byproduct derived from biodiesel production, is a biodegradable natural plasticizer. Deionized (DI) water served as a processing solvent—subsequently removed during later steps—and facilitated the formation of hydrogen bonds and disulfide linkages between glutenin and gliadin of the gluten proteins.

WG-vegan leather was fabricated by compression & molding method according to following steps. First, WG powder was sieved into uniform particles by a fine mesh sieve (pore size: 100 μm). Then WG powder (30 g), glycerol (15 wt.% of WG), and DI water (15 mL) were mixed in a planetary mixer (PLM-0.6K, DAEWHA Tech Co., Ltd, Korea) with two twist type blades at 150 rpm for 5 min. The obtained dough was subjected to heat (60 °C) and pressure (5 MPa) for 90 s using a hot press machine (QM900SA, QMESYS, Korea), and was molded into a film with a thickness of 1.5 mm. Then, the surface of the WG film was exposed to 254 nm UV light (VL-6.LC, VILBER) for 1 h (6W powder) and heated at 150°C for 5 minutes and subsequently. After that, the WG-leather was left in an oven at 30 °C overnight.

## Characterization

### Leather-like Physical Performance

Bovine leather (izleather, Korea), commercial PU leather (YBK, Korea), and commercial rubber (Narabelt, Korea) were used for comparison. Mechanical properties of WG-vegan leathers were measured by UTM (AGS-X Series, SHIMADZU). According to ISO 13934-2:2014 (Tensile properties of fabrics - Determination of maximum force using the grab method), tensile strength and strain were evaluated. The specimen was cut into a dog-bone shape (ISO 37-4) and subjected to mechanical property testing at a pulling speed of 100 $ms^{-1}$. All measurements were performed five times for each sample, and the average values were obtained. The water resistance properties were examined by water contact angle (WCA) and swelling test. First, WCA was analyzed using a contact angle measurement system by the sessile drop method, in which a 2 μL droplet of deionized water was placed on the surface of each sample using a micropipette at a suitable distance to the testing platform. The angle formed by the tangent of the droplet with the surface of each sample was recorded by digital camera (38MP FHD Camera V6). The average WCA value was obtained by measuring five different spots on the surface of each sample. Next, the swelling ratio was measured according to ASTM D471. The test specimen was prepared by cutting it into a standard size (e.g., 25x25 $mm^2$ with a thickness of 2-3 mm) and measuring its initial weight. The specimen was then immersed in water at room temperature for 24 h. After immersion, the specimen was removed, gently blotted to remove surface water, and its weight was measured again. The percentage change in mass was calculated to evaluate the water absorption characteristics of the material. ($W_t$: Weight of the sample after swelling at time $t$, $W_0$: Initial weight of the sample before swelling).

$$\text{Swelling Ratio (\%)} = (W_t - W_0) / W_0 \times 100$$

**Leather-like Texture Evaluation**

The tactile properties were evaluated using a portable tribometer (Heidon, Portable Friction Meter, 94i-II, Japan). For skin friction measurements, ten participants were involved. Prior to testing, their forearm skin was cleansed with a tissue soaked in 70% ethanol to remove sweat and dirt, followed by a one-minute drying period. Friction values were recorded at ten different points on the forearm, and the average value was calculated. To assess the friction between bovine leather or WG-vegan leather and human skin, samples with a thickness of less than 1 mm were affixed to the metal surface of the tribometer's sensor. Measurements were then taken at ten different positions on the randomly selected participant's forearm.

Then, the vertical elasticity (Shore A hardness) test was conducted in accordance with ISO 868:2003. The specimen was prepared by stacking three layers of 1.5 mm thick samples to achieve the required thickness and was conditioned under standard testing conditions. The experiment was performed at a temperature of 23°C and a relative humidity of 30%, using a Shore A durometer HBA 100-0 (SAUTER, Germany). The indenter was positioned perpendicularly to the specimen, and the hardness value was recorded 15 seconds after applying the load.

The lateral elasticity test was conducted following ASTM D1388-18 (Standard Test Method for Stiffness of Fabrics: The Heart Loop Test) with slight modifications.[S1] The sample dimensions were adjusted to 5 × 9 × 10 cm. Each sample was formed into a loop, and after 1 minute, the distance from the upper end to the lowest point of the loop was recorded. The change in distance was then calculated using the following equation.

$$\Delta d(\%) = (d_1 - d_0) / d_0 \times 100$$

($\Delta d$ : the change in the distance, $d_0$ : the distance of the loop before the measurement, $d_1$ : the distance of the loop after 1 min). All measurements were repeated three times.

**Protein Denaturation Analysis**

The surface morphologies and detailed microstructures of the WG-vegan leathers were investigated using scanning electron microscopy (SEM, Hitachi, S-4300SE). All samples were sputter-coated with platinum using a magnetron sputter coater (108auto; Cressington Scientific Instruments, Watford, UK) and then observed at an acceleration voltage of 3 kV. Fourier-transform infrared (FT-IR) spectroscopy was performed using a Bruker VERTEX 80 V spectrometer. A Fourier transform-infrared (FT-IR) spectrometer was used to examine the chemical structures of WG-vegan leathers. The FT-IR spectra of the samples were recorded in the wavenumber range of 650–4000 $cm^{-1}$ at a resolution of 0.4 $cm^{-1}$ with 32 scans. Baseline normalization was carried out for each spectrum using OMNIC software (Thermo Fisher Scientific, MA, USA). X-ray diffraction (XRD, Rigaku, D/MAX 2200V/PC) with Cu-Kα radiation (λ = 0.154056 nm) was performed to evaluate the degree of intermolecular packing and alignment of the WG-vegan leathers. The molecular structures of samples were examined in the 2h range of 0–40 and carried out with a Cu-Ka radiation source (k = 1.5406 nm) at 40 kV and 40 mA.

Free amino acids were analyzed using a Dionex Ultimate 3000 HPLC system (Thermo Scientific, USA) with pre-column derivatization using borate buffer, OPA, and FMOC reagents. Separation was performed on an Inno C18 column (4.6 × 150 mm, 5 μm; YoungJin Biochrom, Korea) at 40°C, using a binary gradient of 40 mM sodium phosphate buffer (pH 7) and a mixture of water/acetonitrile/methanol (10:45:45, v/v) at a flow rate of 1.5 mL/min. Detection was carried out by fluorescence (Ex/Em: 340/450 nm for OPA, 266/305 nm for FMOC) and UV at 338 nm. Samples were prepared by extracting 1 g of sample with 50 mL of 0.1 M perchloric acid and 0.1% meta-phosphoric acid, followed by sonication, shaking, filtration, and automated derivatization. Quantification was based on a 17-component amino acid standard (Agilent).

LC-MS and LC-MS/MS analyses were performed using an Ultimate3000 system (Thermo Scientific, USA) equipped with a Waters Cortecs T3 column (2.1 mm × 150 mm, 1.6 μm, Waters). The column temperature was maintained at 45°C. The mobile phases consisted of solvent A (0.2% formic acid in water) and solvent B (0.2% formic acid in acetonitrile), with a flow rate of 0.25 mL/min. A gradient

elution was applied as follows: 0 min (99% A), 0.5 min (99% A), 25 min (75% A), 32 min (5% A), 35 min (5% A), 35.1 min (99% A), and 40 min (99% A). Mass spectrometric detection was carried out using a Triple TOF 5600+ system (AB Sciex, USA) with electrospray ionization (ESI) in positive mode. Data was acquired in full scan and information-dependent acquisition (IDA) mode. The MS scan range was set to 100–2000 m/z, and the MS/MS scan range was 30–2000 m/z. Source conditions were as follows: ion source gas 1 and 2 (nebulizer and heater gas) at 50 psi, curtain gas at 25 psi, and desolvation temperature at 500°C. The ion spray voltage was set to +5.5 kV, declustering potential (DP) at 60 V, collision energy (CE) at 10 V, and collision energy spread (CES) at 35 ± 15 V. Nitrogen ($N_2$) was used as the collision gas.

Fluorescence microscope images were obtained using a Leica Thunder Imager equipped with a K8 CMOS camera (Leica Microsystems, Wetzlar, Germany) and controlled by LAS X software. To compare the film before and after surface treatment, fluorescence was captured under the following conditions: blue channel (excitation 390 nm/emission 420–460 nm), green channel (excitation 475 nm/emission 490–530 nm), yellow channel (excitation 560 nm/emission 565–615 nm), and red channel (excitation 635 nm/emission 662–738 nm). All images were acquired using a 5× objective lens, with an exposure time of 50 ms and LED power set to 20%.

**Environmental Impacts**

Life cycle assessment (LCA) was conducted using the *openLCA* (version 2.4.1) with the ecoinvent 3.11 database (cut-off system model). The analysis was performed across five key processes: (1) gluten extraction, (2) gluten dough processing, (3) hot pressing, (4) surface treatment, and (5) oven drying. The electricity consumption of each process was measured using a power meter (Seojun Co., Ltd., South Korea) and is presented in Table S4. The ecoinvent datasets used in this study include wheat flour, deionized water, glycerin, and medium voltage electricity (cutoff). The climate change-global warming potential (GWP100) was selected as the impact category, and the final product was assessed on a per 1 kg basis using the IPCC impact assessment method. The energy recovery values used in Scenario 3

were based on the data reported by *Yelin Deng, 2013*.

To investigate the biodegradability of WG-vegan leather, we conducted a bio-decomposition test following the ISO 20200 standard method. Sample films with a thickness of 1.5 mm into 25 × 25 $mm^2$ pieces and weighed them for four replicates. Prepared sample films were inserted at a depth of 4–6 cm in perforated plastic boxes filled with compost consisting of sawdust (40%), rabbit feed (30%), ripe compost (10%), corn starch (10%), saccharose (5%), corn seed oil (4%), and urea (1%), under controlled conditions of 58°C and 55% humidity. At various time points (1,2,3,4,5,6, and 7 week), the samples were retrieved to assess their disintegration. The degree of disintegration (*D*) was calculated by using the following equation: $D = (m_i - m_r / m_i) \times 100$ where $m_i$ is the initial dried sample mass, and $m_r$ is the dried sample mass after the test.

Superworms edibility test was adapted from the protocol reported by Jung et al. Superworms in their larvae stage (*Z. atratus*) were acquired from a local supplier (Mealworm Nara, Yeoju, Korea), with a length ranging from 5 to 6 cm. Prior to the feeding, the superworms were subjected to a 36h starvation period. In a polypropylene container (D x H = 103 x 78.6 mm), a total of 30 superworms were fed WG-heat film, WG-UV film, WG-leather as their exclusive diet respectively. For comparative purposes, three control groups were set up: the first group was fed with bran, a feed widely used for superworms; the second group was intentionally left unfed to induce a state of starvation; and the third group received biodegradable plastics PLA & PBAT (Lotte Chemical, Korea). The superworms were incubated for 4 weeks at 26 ± 1 ◦C. To replace moisture, deionized water was provided, and dead superworms were removed immediately. The superworm survival rate, body weight changes, and plastic consumption were recorded every day. All treatments were carried out in triplicate.

**Table S1. Sample name**

| Sample | WG (g) | GL (g) | DI water (ml) | TA (g) | $FeCl_2$ (g) | Surface treatment | 6M HCl hydrolysis |
|---|---|---|---|---|---|---|---|
| **WG-film (GL10)** | 30 | 3 | 15 | - | - | - | - |
| **WG-film, WG-film (GL15)** | 30 | 4.5 | 15 | - | - | - | - |
| **WG-film (GL20)** | 30 | 6 | 15 | - | - | - | - |
| **WG-film (GL25)** | 30 | 7.5 | 15 | - | - | - | - |
| **WG-film (brown)** | 30 | 4.5 | 15 | 0.9 | - | - | - |
| **WG-film (darkbrown)** | 30 | 4.5 | 15 | 0.9 | 0.3 | - | - |
| **WG-film (black)** | 30 | 4.5 | 15 | 0.3 | 0.9 | - | - |
| **WG-film (2h)** | 30 | 4.5 | 15 | - | - | X | 2h |
| **WG-film (24h)** | 30 | 4.5 | 15 | - | - | X | 24h |
| **WG-leather (2h)** | 30 | 4.5 | 15 | - | - | O | 2h |
| **WG-leather (24h)** | 30 | 4.5 | 15 | - | - | O | 24h |

**Table S2. Tensile strength and elongation at break of different leathers (Ashby's plot)**

| Sample | | Tensile strength (MPa) | | Elongation at break (%) | |
|---|---|---|---|---|---|
| | | Avg. | SD | Avg. | SD |
| WG-vegan leather | WG-film (GL10%) | 14.8 | 4.43 | 23 | 2.45 |
| | WG-film, WG-film (GL15%) | 10.1 | 3.45 | 68 | 3.33 |
| | WG-film (GL20%) | 7.6 | 2.34 | 106 | 3.78 |
| | WG-film (GL25%) | 4.2 | 2.33 | 135 | 3.67 |
| | WG-leather | 12.1 | 1.65 | 64 | 5.75 |
| | WG-leather (brown) | 15.2 | 2.45 | 56 | 2.57 |
| | WG-leather (dark brown) | 16.7 | 3.31 | 51 | 3.67 |
| | WG-leather (black) | 17.2 | 2.55 | 44 | 4.32 |
| Bovine leather | | 17.9 | 2.65 | 58 | 3.78 |
| Commercial PU leather | | 8.4 | 3.34 | 62 | 4.65 |
| Alternative leather | Pinatex®[21] | 4.5 | - | 30 | - |
| | Muskin®[21] | 0.2 | - | 48 | - |
| | Desserto®[23] | 9.48 | - | 16 | - |
| | Kombucha leather[22] | 1.69 | 0.33 | 15 | - |
| Solvent casted WG-film | WG film[24] | 0.4 | 0.2 | 160 | 23 |
| | WGP film[25] | 1.75 | - | 90 | - |

**Table S3. Amino-acid composition (HPLC) of WG-dough, WG-film and WG-leather**

| Amino acid (%) | WG-dough | WG-film | WG-leather |
|---|---|---|---|
| Aspartic acid/Asparagine | 2.7 | 2.82 | 2.78 |
| Threonine | 3.23 | 3.08 | 3.47 |
| Serine | 5.5 | 5.15 | 5.41 |
| Glutamic acid/ Glutamine | 34.62 | 27.53 | 34.06 |
| Glycine | 3.73 | 3.91 | 3.07 |
| Alanine | 3.73 | 6.75 | 2.53 |
| Cystine | 1.27 | 3.45 | 1.89 |
| Valine | 5.25 | 6.28 | 4.59 |
| Methionine | 1.31 | 0.47 | 1.61 |
| Isoleucine | 3.55 | 1.76 | 4.46 |
| Leucine | 6.69 | 7.04 | 7.65 |
| Tyrosine | 3.24 | 3.02 | 2.12 |
| Phenylalanine | 3.98 | 5.6 | 5.83 |
| Histidine | 2.97 | 3.28 | 2.7 |
| Lysine | 1.74 | 1.91 | 1.05 |
| Arginine | 2.67 | 2.92 | 4.23 |
| Proline | 13.82 | 15.03 | 12.55 |
| **Total** | **100** | **100** | **100** |

## Table S4. LCA data

*<Scenario 1>*

| Process | Detail index | Energy consumption (kWh) | GWP 100 (kg $CO_2$ eq) |
|---|---|---|---|
| 1. Gluten extraction | cultivation, flour production, gluten separation, drying of 740g gluten powder *(Yelin Deng, 2013)* | - | 1.16 |
| 2. Planetary mixing | planetary mixing with gluten, glycerol, and deionized water | 0.08 | 0.32 |
| 3. Hot pressing | hot press gluten dough to gluten film | 2.52 | 0.05 |
| 4. Surface treatment | heating, UV irradiation to gluten film | 2.92 | 0.06 |
| 5. Oven drying | oven dry for 5 days | 1.51 | 0.03 |
| **Total** | | | **1.63** |

*<Scenario 2>*

| Process | Detail index | Energy consumption (kWh) | GWP 100 (kg $CO_2$ eq) |
|---|---|---|---|
| 1. Planetary mixing | planetary mixing with gluten, glycerol, and deionized water | 0.08 | 0.32 |
| 2. Hot pressing | hot press gluten dough to gluten film | 2.52 | 0.05 |
| 3. Surface treatment | heating, UV irradiation to gluten film | 2.92 | 0.06 |
| 4. Oven drying | oven dry for 5 days | 1.51 | 0.03 |
| **Total** | | | **0.47** |

*<Scenario 3>*

| Process | Detail index | Energy consumption (kWh) | GWP 100 (kg $CO_2$ eq) |
|---|---|---|---|
| 1. Gluten extraction | cultivation, flour production, gluten separation, drying of 740g gluten powder *(Yelin Deng, 2013)* | - | 1.16 |
| 2. Planetary mixing | planetary mixing with gluten, glycerol, and deionized water | 0.08 | 0.32 |
| 3. Hot pressing | hot press gluten dough to gluten film | 2.52 | 0.05 |
| 4. Surface treatment | heating, UV irradiation to gluten film | 2.92 | 0.06 |
| 5. Oven drying | oven dry for 5 days | 1.51 | 0.03 |
| 6. Energy recovery | incineration with energy recovery *(Yelin Deng, 2013)* | | -0.078 |
| **Total** | | | **1.55** |

The GWP100 values for each process in Scenario 1 were calculated using the openLCA software in conjunction with the Ecoinvent 3.11 dataset. In Scenario 2, the Gluten extraction stage was excluded, resulting in a calculated value of 0.47 kg $CO_2$-eq (1.63 – 1.16 = 0.47 kg $CO_2$-eq). For Scenario 3, the energy recovery value reported by Deng (2013) was applied, subtracting 0.078 kg $CO_2$-eq from 1.63 kg $CO_2$-eq, yielding a result of 1.55 kg $CO_2$-eq.

**Figure S1. S-S curve of WG-vegan and other leathers**

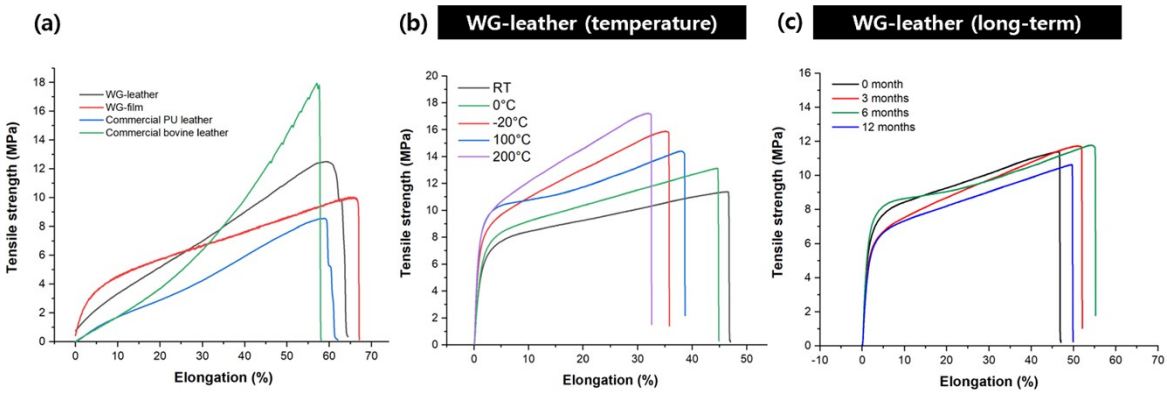


S-S curves of (a) different types of leathers (b) WG-leathers at different temperatures (c) WG-leathers after long-term storage

The stress–strain curves of commercial bovine leather, commercial PU leather, and WG-based vegan leather (WG-film and WG-leather) were compared. Despite the decrease in modulus, WG-leather retained a high toughness value (4.65 $MJ \cdot m^{-3}$), slightly exceeding that of WG-film (4.58 $MJ \cdot m^{-3}$) and considerably higher than that of commercial PU leather (2.72 $MJ \cdot m^{-3}$). These results indicate that the physical surface treatment effectively tuned the mechanical properties of WG-film to achieve leather-like flexibility, while maintaining superior energy absorption performance compared to conventional PU leather.

Considering the practical conditions where WG-leather may be exposed to both elevated and sub-zero temperatures, as well as prolonged storage under ambient environments, it was necessary to evaluate its mechanical reliability under these realistic scenarios. The temperature exposure tests were conducted by storing the samples in an oven at 100 °C and 200 °C, as well as in a refrigerator (0 °C) and a freezer (–20 °C) for three days, followed by mechanical property measurements. The results showed that, compared to room temperature, both high- and low-temperature storage led to increased tensile strength and decreased elongation due to additional curing. This indicates that the WG-leather exhibits a tensile strength of approximately 17 MPa, comparable to that of natural leather, and maintains its mechanical integrity without degradation even after storage under both high and low temperatures (Figure S1. (b)).

Additionally, to examine the long-term stability of WG-leather, UTM measurements were

conducted after storage at room temperature for 0, 3, 6, and 12 months. For the long-term storage test, WG-leather samples were kept in a low-density polyethylene (LDPE) bag without desiccants at room temperature (RT) before measurement. The tensile strength slightly increased up to 6 months and then showed a minor decrease after 12 months. Since these variations remained within 10% of the initial tensile strength, the WG-leather is considered to maintain stable mechanical properties during long-term storage (Figure S1. (c)).

**Figure S2. Physical & tactile properties of various leathers**

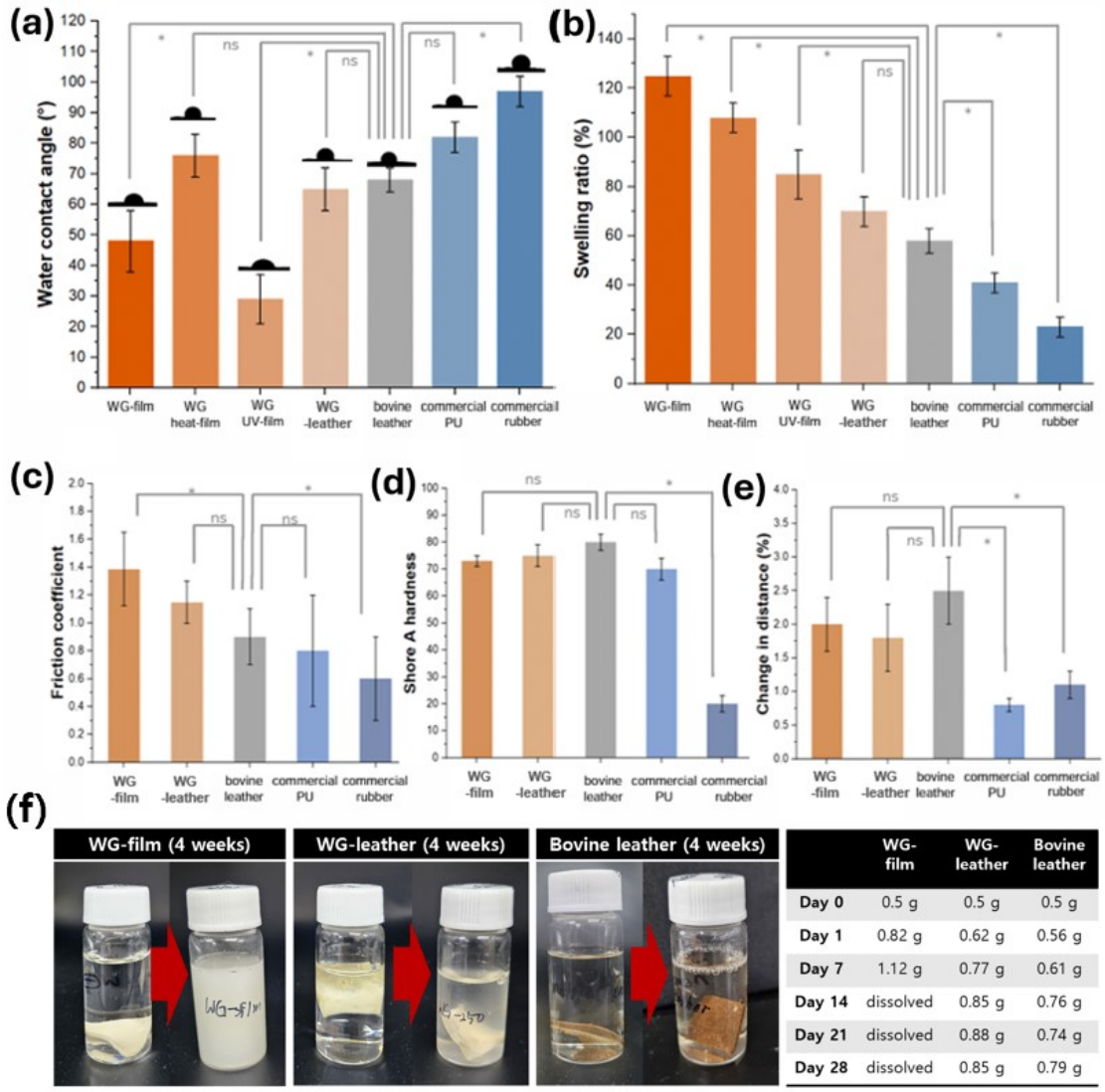


| | WG-film | WG-leather | Bovine leather |
|---|---|---|---|
| Day 0 | 0.5 g | 0.5 g | 0.5 g |
| Day 1 | 0.82 g | 0.62 g | 0.56 g |
| Day 7 | 1.12 g | 0.77 g | 0.61 g |
| Day 14 | dissolved | 0.85 g | 0.76 g |
| Day 21 | dissolved | 0.88 g | 0.74 g |
| Day 28 | dissolved | 0.85 g | 0.79 g |

(a) Water contact angle, (b) swelling ratio, (c) friction coefficient, (d) shore A hardness, (e) heart loop test (f) long-term swelling test of various leathers (The error bars indicate the standard deviation (SD) of the mean (n = 3) and statistical significance was determined using unpaired two-tailed t-tests. $p \leq 0.05$ (*), $p \leq 0.01$ (**), and $p > 0.05$ (ns, not significant))

We performed a long-term swelling test comparing WG-film, WG-leather, and bovine leather. Prior to testing, the surface of bovine leather was gently abraded with sandpaper to eliminate the effects of surface synthetic polymer coatings. After one month of water immersion, the WG-film completely dissolved, whereas both WG-leather (denatured) and uncoated bovine leather remained structurally intact without visible degradation. The uncoated bovine leather exhibited a swelling ratio of approximately 60%, comparable to that of WG-leather, confirming that the surface treatment

substantially enhanced the water resistance of the WG-leather. This level of water resistance is comparable to that of bovine leather, and it could be further improved by introducing sustainable hydrophobic coatings.[S6]

**Figure S3. Different colors of WG-leather as a result of the pyrogallol-based natural product coating.**

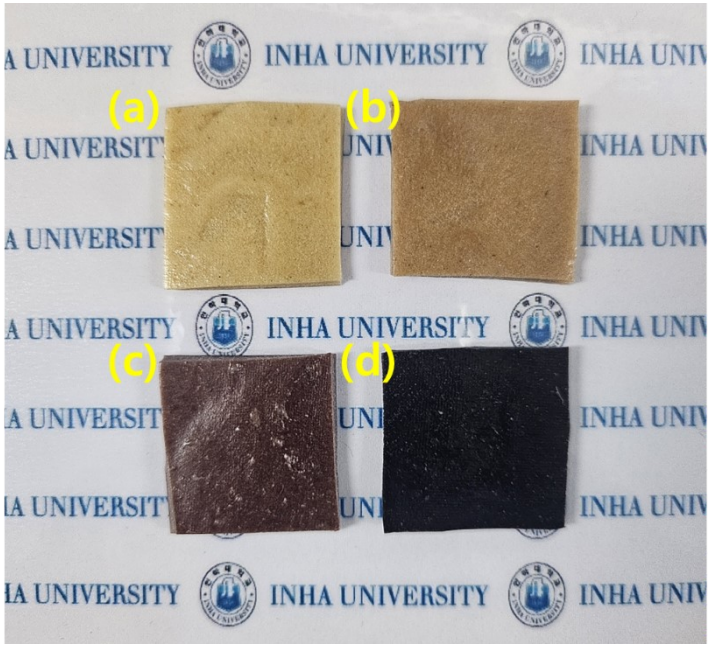


(a) WG-leather (b) WG-brown (C) WG-darkbrown (d) WG-black

The dyeing process was conducted to impart various colors to WG-leather. Utilizing nature-derived tannic acid and iron(III) chloride, the beige WG-leather was dyed to achieve brown, gray, and black colors. These solutions were incorporated into the WG-leather in place of deionized water before planetary mixing, resulting in various colors. Tannic acid is a natural pyrogallol compound and is derived from plants. tannic acid and iron(III) chloride have been traditionally utilized as dye and ink ingredients, and the methodology is well established. Thanks to the hydrophilicity and miscibility of the WG material, the samples were dyed homogeneously and well.

**Figure S4. Optical microscopy (OM) image of WG-film & WG-leather**

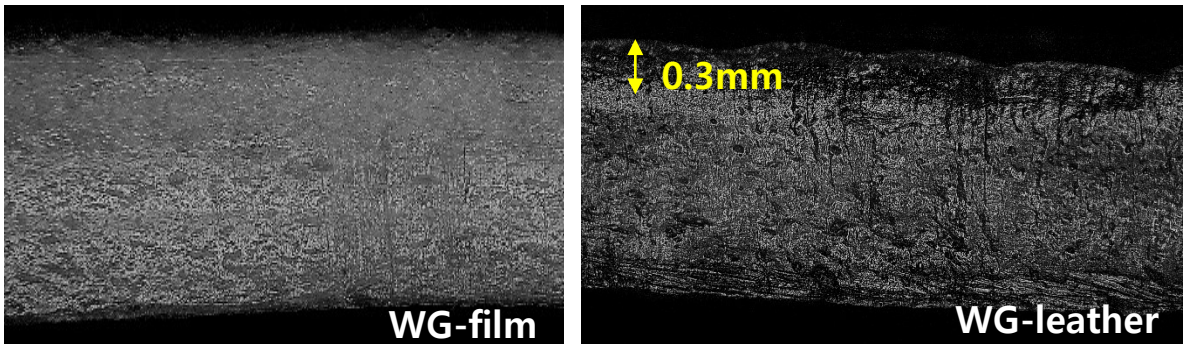


Cross-sectional imaging was conducted using optical microscopy (OM) to compare the WG-film and WG-leather. In the WG-leather, which was subjected to additional high-temperature treatment and UV irradiation, a distinct coating layer approximately 0.3 mm thick was observed on the surface. In contrast, no such coating layer was present in the untreated WG-film. The formation of this coating layer is believed to have contributed to the enhanced hydrophobicity and water resistance of WG-leather.

**Figure S5. XRD**

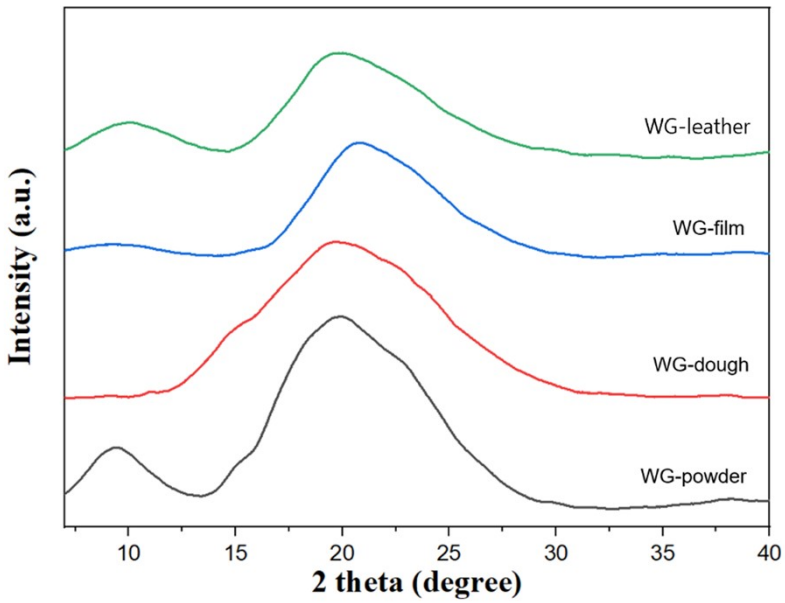


XRD analysis was conducted to investigate the changes in the molecular structure of WG-powder, WG-dough, WG-film, and WG-leather under varying heat and pressure. In WG-powder, two broad peaks were observed around 10° and 20°, with full width at half maximum (FWHM) values of 3.07 and 7.46, respectively.[S2] When mixed with glycerol and water to form WG-dough, the peak around 10°C has disappeared, with an increased FWHM of 9.53. This suggests that the original structure of gluten protein powder, with glutenin and gliadin arranged in an ordered manner, was reduced upon random mixing with plasticizers and water, resulting in an amorphous structure formed through disulfide and hydrogen bonds. In WG-film, two peaks emerged, both with an FWHM of 7.21, indicating the formation of a new structure. This recovery likely resulted from reduced molecular spacing and more ordered arrangements within the gluten complex under heat and pressure. Finally, WG-leather exhibited a general trend of reduced FWHM, with a value of 3.69 and 7.17, respectively. This suggests that additional surface heat treatment decreased hydrogen bonding between water and glycerol while increasing hydrogen bonding with proteins, leading to enhanced stability and the formation of a new structure.

**Figure S6. FT-IR**

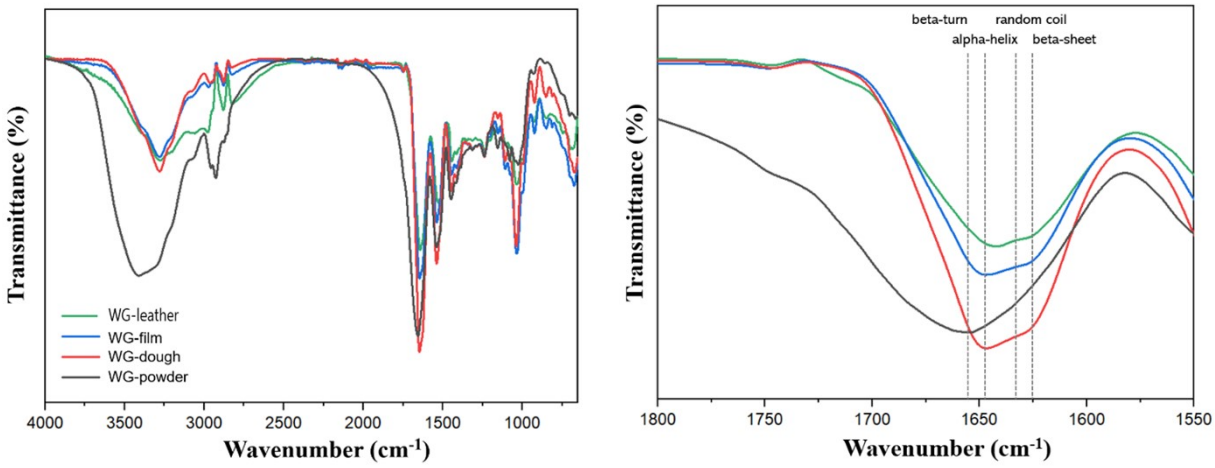


FT-IR analysis was conducted to examine changes in the secondary structure of proteins in WG-vegan leathers. The N-H stretching peak (3200–3500 $cm^{-1}$) was most prominently observed in WG powder, which is attributed to the amine groups present at the terminal ends of amino acids. These peaks decreased as the process progressed, likely due to the formation of hydrogen bonds and other types of binding. Similarly, the O-H stretching peak (3200–3600 $cm^{-1}$) showed a decreasing trend upon heat treatment, which can be attributed to the evaporation of water and glycerol caused by compression and heat treatment. The C-H stretching peak was primarily observed in peaks abundant in sp3 carbons from gluten proteins. If carbonization had occurred due to heat treatment, peaks corresponding to C=C (1620-1680 $cm^{-1}$) and C≡C (1450-1600 $cm^{-1}$) would have formed. Therefore, it can be concluded that carbonization did not take place.

In the amide I region (right side; 1550-1800 $cm^{-1}$), the beta-turn and alpha-helix peaks were dominant in WG powder, while beta-sheet peak was scarcely observed. However, as WG transformed from powder to dough, film, and leather, the beta-sheet peak increased, whereas the beta-turn and alpha-helix peaks showed a decreasing trend[S3]. It suggests the formation of a more stabilized and ordered layered configuration through protein denaturation by thermal and UV treatments. Moreover, the overall peaks in the amide I region exhibited a red shift, reflecting changes in the hydrogen bonding environment and the reorganization of protein secondary structures during the transformation process.

**Figure S7. 2h, 24h protein hydrolysis scheme and LC-MS/MS data**

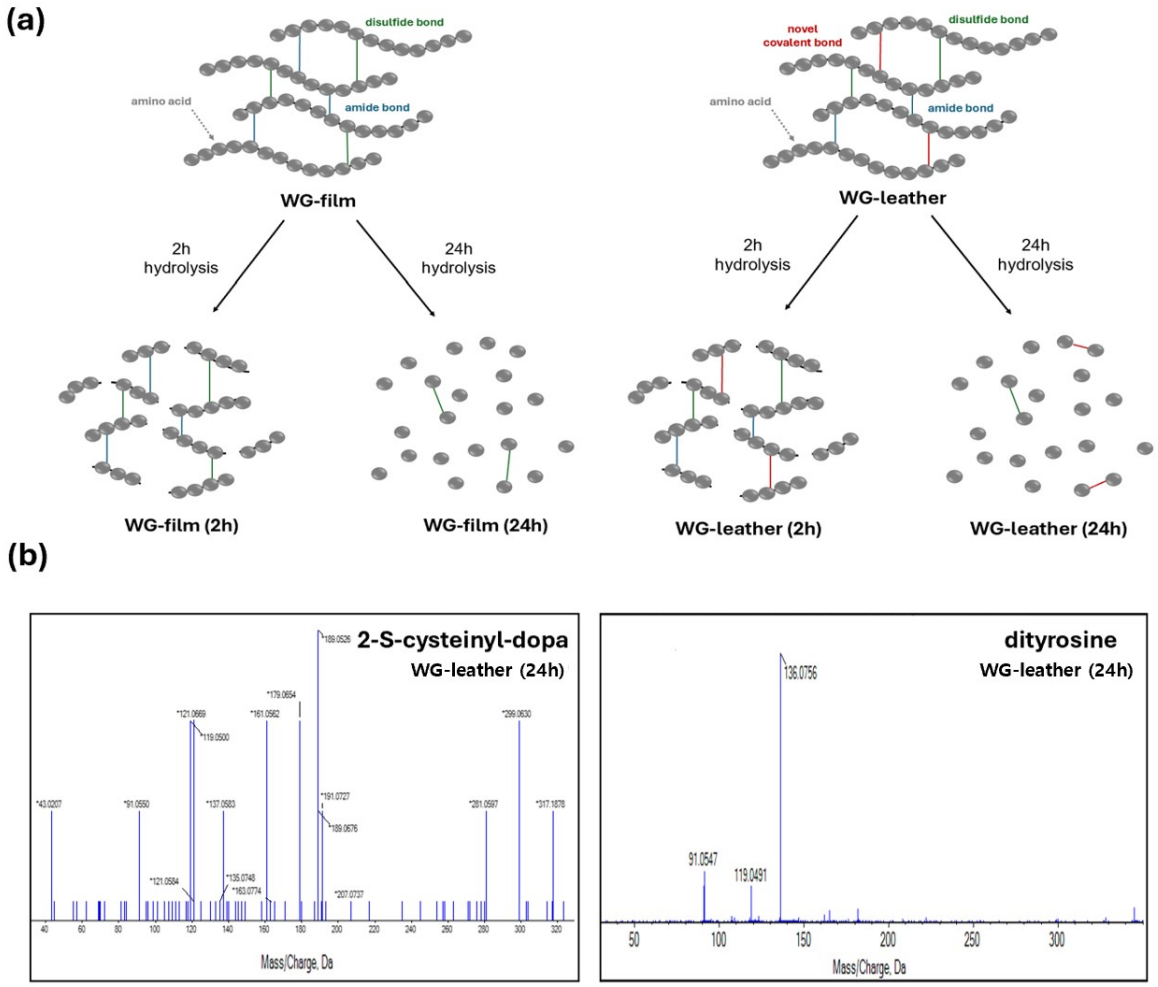


(a) WG-leather hydrolysis scheme
(b) LC-MS/MS spectrum of different compounds in WG-leather (24h)

LC-MS/MS analysis was conducted on WG-film (untreated) and WG-leather (surface-treated) after 2-hour and 24-hour 6M HCl hydrolysis. Assuming that both the 24-hour hydrolyzed WG-film and WG-leather were completely broken into amino acid fragments, the remaining strong cross-linked structures were subsequently identified. 2-S-cysteinyl-DOPA and dityrosine—absent in WG-film—were identified in WG-leather and remained detectable even after prolonged hydrolysis.

**Figure S8. Soil degradation (ISO 20200)**

Soil biodegradation of PLA, PBAT, WG-heat film, WG-UV film, and WG-leather (7 weeks)

**Figure S9. Superworms edibility test**

Superworms edibility test of PLA, PBAT, WG-heat film, WG-UV film, and WG-leather (14 days)

**Figure S10. XPS analysis of WG-dough, WG-film and WG-leather**

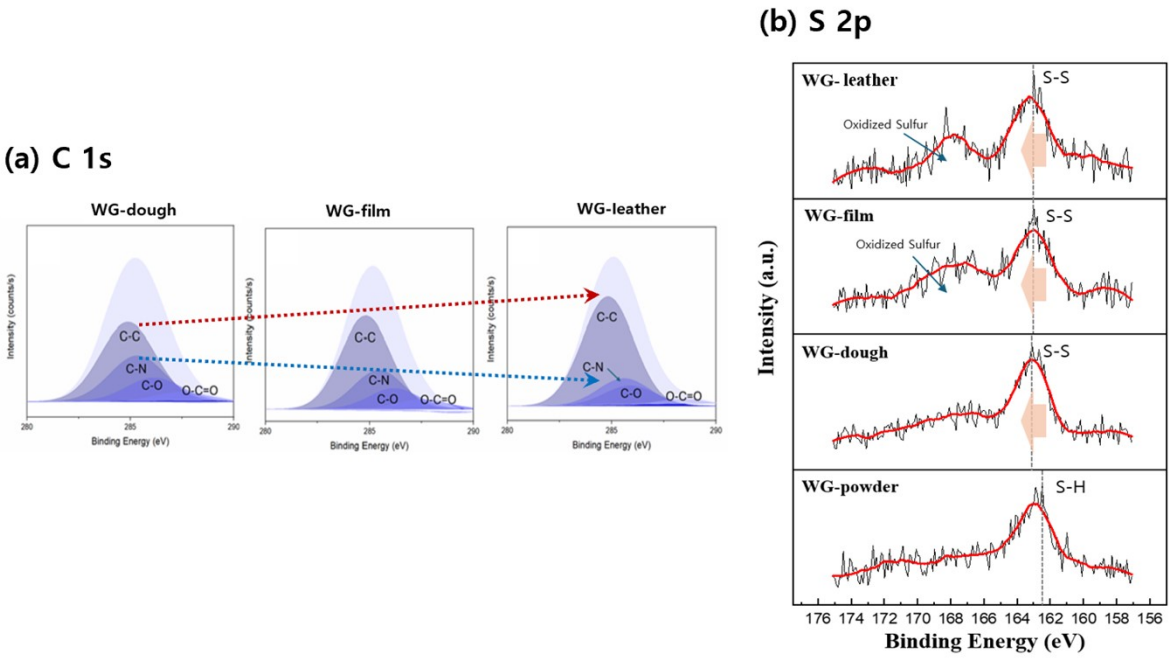


(a) C 1s (b) S 2p XPS analysis of WG-dough, WG-film and WG-leather

To examine the respective effects of heat and UV treatment, we performed XPS analyses on gluten-dough, gluten-film, and gluten-leather samples. In the S 2p spectra, a relatively low sulfur intensity was observed; however, progressive heat and UV treatments led to the formation of oxidized sulfur species (166–170 eV) and a peak shift from the –SH signal (162 eV) to the disulfide (S–S) bond region (163 eV).[S7] In the C 1s spectra, the heat-treated WG-film exhibited a decrease in C–N bonding and an increase in C–C bonding, and these trends became more pronounced in the UV-treated WG-leather.[S8] These results support that the surface treatment of WG-leather induced a reduction in C–N (amide) bonds and an increase in C–C (covalent) bonds, accompanied by the formation and oxidation of disulfide bonds in sulfur.

**Movie S1. Elastic recovery test of bovine, PU and WG-leather**

The video included the elastic recovery behavior of natural leather, synthetic PU leather, and gluten-based leather. Natural leather exhibited quick elasticity with a recovery time of approximately 0.8 seconds, attributed to its fibrous collagen structure, which enables rapid elastic recovery. In contrast, synthetic PU leather showed a slow recovery time of 2.3 seconds, likely due to its composite structure incorporating nonwoven substrates and multiple laminated layers, which limit its ability to return quickly to its original form. The gluten-based leather demonstrated an elastic recovery time of 2.0 seconds, showing a recovery profile closer to that of natural leather than PU leather, suggesting its promise as a sustainable alternative with favorable tactile and functional properties.

## Supporting references


S1. H. Kim, J. E. Song and H. R. Kim, *Cellulose*, **2021**, *28*, 3183–3200, DOI: 10.1007/s10570-021-03705-0.

S2. N. Leblanc, R. Saiah, E. Beucher, R. Gattin, M. Castandet and J.-M. Saiter, *Carb. Polym.* (Carbohydrate Polymers), **2008**, *73*, 548–557, DOI: 10.1016/j.carbpol.2007.12.034.

S3. D. M. R. Georget and P. S. Belton, *Biomacromolecules*, **2006**, *7*, 469–475, DOI: 10.1021/bm050667j.

S4. Y. Deng, W. M. J. Achten, K. Van Acker and J. R. Duflou, *Biofuels Bioprod. Bioref.*, **2013**, *7*, 429–458, DOI: 10.1002/bbb.1406.

S5. S. Boonyod, W. Pivsa-Art, P. Nanthananon, Y. K. Kwon and S. Pivsa-Art, *J. Polym. Environ.*, **2023**, *31*, 3070–3080, DOI: 10.1007/s10924-023-02804-2.

S6. J. Ryu, L. T. Hao, H. Kim, S. Lee, H. Jeon, D. S. Hwang, J. Park, C. H. Park, D. X. Oh, J. M. Koo and S. B. Park, ACS Sustainable Chem. Eng., **2025**, 13, 7585–7597, DOI: 10.1021/acssuschemeng.5c01838.

S7. B. Chen, Y. Cao, Q. Li, Z. Yan, R. Liu, Y. Zhao, X. Zhang, M. Wu, Y. Qin, C. Sun, W. Yao, Z. Cao, P. M. Ajayan, M. O. L. Chee, P. Dong, Z. Li, J. Shen and M. Ye, Nat. Commun., **2022**, 13, 1206, DOI: 10.1038/s41467-022-28901-9.

S8. M. C. Wehrli, T. Kratky, M. Schopf, K. A. Scherf, T. Becker and M. Jekle, Int. J. Biol. Macromol., **2021**, 173, 26–33, DOI: 10.1016/j.ijbiomac.2021.01.008.